Journal of Cancer Research and Clinical Oncology (2024) 150:483
https://doi.org/10.1007/s00432-024-06008-6

RESEARCH

Prognostic nomogram model based on quantitative metrics of subregions surrounding residual cavity in glioblastoma patients

Lijuan Gao[1] · Tao Yuan[1] · Yawu Liu[2,3] · Xiaoyun Yang[4] · Yiming Li[5] · Guanmin Quan[1]

Received: 5 June 2024 / Accepted: 22 October 2024

Abstract

Background The hyperintensity area surrounding the residual cavity on postoperative fluid-attenuated inversion recovery (FLAIR) image is a potential site for glioblastoma (GBM) recurrence. This study aimed to develop a nomogram using quantitative metrics from subregions of this area, prior to chemoradiotherapy (CRT), to predict early GBM recurrence.

Methods Adult patients with GBM diagnosed between October 2018 and October 2022 were retrospectively analyzed. Quantitative metrics, including the mean, maximum, minimum, median values, and standard deviation of FLAIR signal intensity (SI) (measured using 3D-Slicer software), were extracted from the following subregions surrounding the residual cavity on post-contrast T1-weighted (CE-T1WI)-FLAIR fusion images: the enhancing region (ER), non-enhancing region (NER), and combined ER + NER. Independent prognostic factors were identified using Cox regression and least absolute shrinkage and selection operator (LASSO) analyses and were incorporated into the prediction nomogram model. The model's performance was evaluated using the C-index, calibration curves, and decision curves.

Results A total of 129 adult GBM patients were enrolled and randomly assigned to a training (n = 90) and a validation cohorts (n = 39) in a 7:3 ratio. Sixty-nine patients experienced postoperative recurrence. Cox regression analysis identified subventricular zone involvement, the median FLAIR intensity in the ER, the rFLAIR (relative FLAIR intensity compared to the contralateral normal region) of ER + NER, and corpus callosum involvement as independent prognostic factors. For predicting recurrence within 1 year after surgery, the nomogram model had a C-index of 0.733 in the training cohort and 0.746 in the validation cohort. Based on the nomogram score, post-operative GBM patients could be stratified into high- and low-risk for recurrence.

Conclusions Nomogram models which based on quantitative metrics from FLAIR hyperintensity subregions may serve as potential markers for assessing GBM recurrence risk. This approach could enhance clinical decision-making and provide an alternative method for recurrence estimation in GBM patients.

Keywords Glioblastoma · Magnetic resonance imaging · Postoperative · Nomogram · Recurrence

✉ Yiming Li
57710441@qq.com

✉ Guanmin Quan
quanguanmin@hebmu.edu.cn

[1] Department of Medical Imaging, The Second Hospital of Hebei Medical University, Shijiazhuang 050000, China

[2] Department of Radiology, Kuopio University Hospital, Kuopio, Finland

[3] Department of Neurology, University of Eastern Finland, Kuopio, Finland

[4] Department of Ultrasound, The Second Hospital of Hebei Medical University, Shijiazhuang, China

[5] College of Hebei Medical University, Shijiazhuang, China

Abbreviations

GBM	Glioblastoma
CRT	Chemoradiotherapy
FLAIR	Fluid-attenuated inversion recovery
CE-T1WI	Contrast-enhancement T1-weighted
ER	Enhanced regional outside the residual cavity
NER	Non-enhancement region outside the residual cavity
LASSO	Least absolute shrinkage and selection operator
NCCN	National Comprehensive Cancer Network
RANO	Response assessment in neuro-oncology
KPS	Karnofsky performance status
PFS	Progression-free survival
OS	Overall survival

Published online: 01 November 2024

PACS	Picture Archiving and Communication System
SVZ	Sub-ventricular zone
MAR	Maximum area ration
SI	Signal intensity
ROI	Regions of interest
ICC	Intraclass correlation coefficient
VIFs	Variance inflation factors
ROC	Receiver operating characteristic
AUC	Area under the curve
MRS	MR Spectroscopy
DWI	Diffusion weighted imaging
PWI	Perfusion weighted imaging
DTI	Diffusion tensor imaging

Introduction

Glioblastoma (GBM) is the most common histological subtype of gliomas and is typically associated with poor outcomes. Its aggressive nature often leads to recurrence within a year of diagnosis (Zhang et al. 2024; Behling et al. 2022). While novel treatments, including immunotherapy and immune-targeted therapy, have shown promise in improving GBM survival, assessing therapeutic efficacy and predicting imminent recurrence before treatment initiation are critical for selecting and promptly implementing salvage therapies.

MRI is the most commonly used imaging modality for assessing GBM post-treatment. However, conventional MRI sequences, such as T2-weighted imaging (T2WI), fluid-attenuated inversion recovery (FLAIR), and contrast-enhanced T1-weighted imaging (CE-T1WI), struggle to accurately characterize the peri-residual cavity region. This underscores the need for quantitative metrics as non-invasive biomarkers for early GBM recurrence detection in the immediate postoperative phase. Accurately characterizing the area surrounding the residual cavity, including FLAIR hyperintensity and enhancement lesions, remains challenging. Additionally, there is considerable variability in the literature regarding assessment timing, region of interest (ROI), and extracted metrics. Some studies focus solely on pre- or post-chemoradiotherapy (CRT) MRI assessments (García Vicente et al. 2022; Rao et al. 2022), overlooking the prognostic impact of surgical factors. In other studies, GBM patients were often dichotomized based on endpoint events, which makes personalized risk assessments difficult. Moreover, there is a lack of comprehensive analysis during the early postoperative stage, such as pre-CRT and immediately after surgery. Recurrence can occur as early as 27 days postoperatively (Behling et al. 2022), and delays in obtaining timely information regarding tumor progression may hinder the initiation of salvage therapy. While recurrence prediction models often rely on MRI morphological features, radiomics, and functional MRI metrics (Wang et al. 2022; Jia et al. 2022), the complexity of the technology and the specialized software required for radiomics hinder widespread clinical use. Thus, traditional MRI remains a cornerstone in prognostic studies of GBM.

Previous studies on post-treatment GBM often employed cluster comparisons, which may overlook individual differences and limit personalized predictions. To enhance the early detection of GBM progression, there is a need for more personalized prediction methods. Nomograms, a simple graphical model, have shown potential in predicting survival outcomes for GBM and other diseases (Huang et al. 2021a, b; Chen et al. 2023). While preoperative MRI-based nomograms have demonstrated predictive value (Du et al. 2022), studies on postoperative MRI nomograms for predicting GBM recurrence before CRT are lacking. Accurately characterizing the FLAIR hyperintensity area surrounding the residual cavity in GBM still remains challenging. This region consists of tumor-infiltrated areas, non-infiltrated areas, and true edema, with the tumor-infiltrated regions being the primary source of GBM recurrence. However, distinguishing these subregions using conventional morphological and conventional functional imaging techniques is difficult. In fact, detecting early signs of recurrence is essential for timely salvage treatment, thus analyzing the FLAIR hyperintensity surrounding the residual cavity may help identify early tumor infiltration. Historically, evaluations of the FLAIR hyperintensity area in glioma patients have focused on size and signal intensity (SI) measurements, which do not adequately reflect the pathophysiological mechanisms in postoperative patients due to lack of differentiation between enhancing and non-enhancing subregions. Previous studies have investigated the FLAIR hyperintensity area with subregion differentiation in preoperative GBM (Yan et al. 2020) and postoperative low-grade glioma patients (Yuan et al. 2022). However, to our knowledge, no studies have emphasized quantitative evaluation and early prediction of GBM recurrence based on subregional analysis of the FLAIR hyperintensity area surrounding the residual cavity. Therefore, further exploration of quantitative subregional analysis for predicting tumor recurrence in postoperative GBM is warranted.

In this study, we developed a novel nomogram model based on the quantitative measurement of subregions within the FLAIR hyperintensity area surrounding the residual cavity before CRT. We further explored how integrating these quantitative metrics with other morphological MRI features and clinical variables could improve the prediction of tumor recurrence.

Methods

Study population and data collection

A retrospective analysis was conducted on GBM patients with complete pathological data who underwent total resection surgery between October 2018 and October 2022. The inclusion criteria were as follows: 1) a confirmed GBM diagnosis according to the 2021 WHO classification of central nervous system tumors, 2) age ≥18 years, 3) tumor located in the cerebral hemisphere; and 4) presence of a single lesion. The exclusion criteria included patients lost to follow-up period, poor quality MRI images, non-adherence to National Comprehensive Cancer Network (NCCN) treatment guidelines, biopsy-only procedures, or death from causes other than GBM. Institutional review board approval was obtained for this study.

Patient data were collected from the hospital information system, including demographics, pathologic diagnosis, treatment strategies, MRI data, and clinical information such as tumor resection and CRT dates, recurrence dates, and postoperative Karnofsky Performance Status (KPS) scores. Pathological data included the Ki-67 proliferation index and molecular phenotypes. According to the response assessment in neuro-oncology (RANO) criteria (Wen et al. 2023), patients with GBM were divided into two groups based on their progression-free survival (PFS) median: those who experienced recurrence within 9 months and those without recurrence within 9 months. GBM recurrence was determined based on specific criteria (Wen et al. 2023). PFS was defined as the time from surgery to recurrence or last follow-up, while overall survival (OS) was defined as the time from surgery to last follow-up or death (Chiang et al. 2020).

Instruments and methodologies

All patients were examined using a Philips Achieva 3.0 T MRI scanner with an 8-channel phased array head coil. For post-contrast scanning, a gadolinium contrast (Gd-DTPA) was administered intravenously at 0.1 mL/kg at 3.0 mL/s, followed by a 20 mL of saline flush. Detailed MRI scan parameters are provided in Table S1. Follow-up MRI examinations were performed within 72 h post-resection, pre-CRT, post-CRT, at the 3-month following surgery, and subsequently at intervals of 3–6 months.

Imaging analysis

MRI data in DICOM format were retrieved from the Picture Archiving and Communication System. Pre-CRT MRI morphological characteristics were assessed, including tumor location, corpus callosum involvement, presence of midline shift, maximum area ratio (MAR) of hyperintensity outside the residual cavity, and the condition of the residual cavity (including morphology, enhancement type, and potential subventricular zone [SVZ] involvement) (Bender et al. 2021). Residual cavity morphology was classified as regular or irregular. The enhancement of the residual cavity wall was categorized into four types: no enhancement, fine line-like enhancement (partial or full wall enhancement <3 mm thick), coarse line-like enhancement (partial or circumferential enhancement 3–5 mm thick), and nodular enhancement (nodules 5–10 mm in diameter) (Wu et al. 2019). The first two types of enhancement were designated as type I, while the latter two were designated as type II. Patients were categorized based on their MAR ratio into residual cavity type (MAR < 1) and edema type (MAR > 1). Further stratification into SVZ+ and SVZ-groups was based on the relationship between the residual cavity and the SVZ (Yamaki et al. 2020).

The workflow of is shown in Fig. 1. The software 3D Slicer (version 5.2.1, https://www.slicer.org/) was used to measure the volume of FLAIR hyperintensity subregions surrounding the residual cavity, including both enhanced and non-enhanced areas. Additionally, the FLAIR SI of hyperintensity subregions at the largest orthogonal cross-section outside the residual cavity was measured using the 3D Slicer software. This analysis included six ROIs, as shown in Fig. 2. The mean, maximum, minimum, and median SI values, along with standard deviation, were directly measured, and relative FLAIR (rFLAIR) values were calculated. The rFLAIR was defined as (ROI-background)/(normal-background) (Yuan et al. 2022). Two radiologists with 6 and 21 years of experience in diagnostic imaging reviewed all findings, with any discrepancies resolved through consultation with a third radiologist with 31 years of neuroradiology experience.

Modeling and evaluation

Cox regression analysis was performed to identify significant factors associated with GBM recurrence. Significant variables from the univariate analysis were included in the multivariate analysis to construct PFS nomograms for predicting recurrence at 6 months and 1 year using software from Jing Ding Medical Technology Co., Ltd. The nomogram's predictive ability was assessed using the C-index, while calibration curves and decision curves were used to evaluate its diagnostic performance. The decision curves plotted net benefit on the vertical axis and threshold probability on the horizontal axis. Kaplan–Meier survival analysis and the log-rank test were used to compare recurrence rates between high- and low-risk groups.

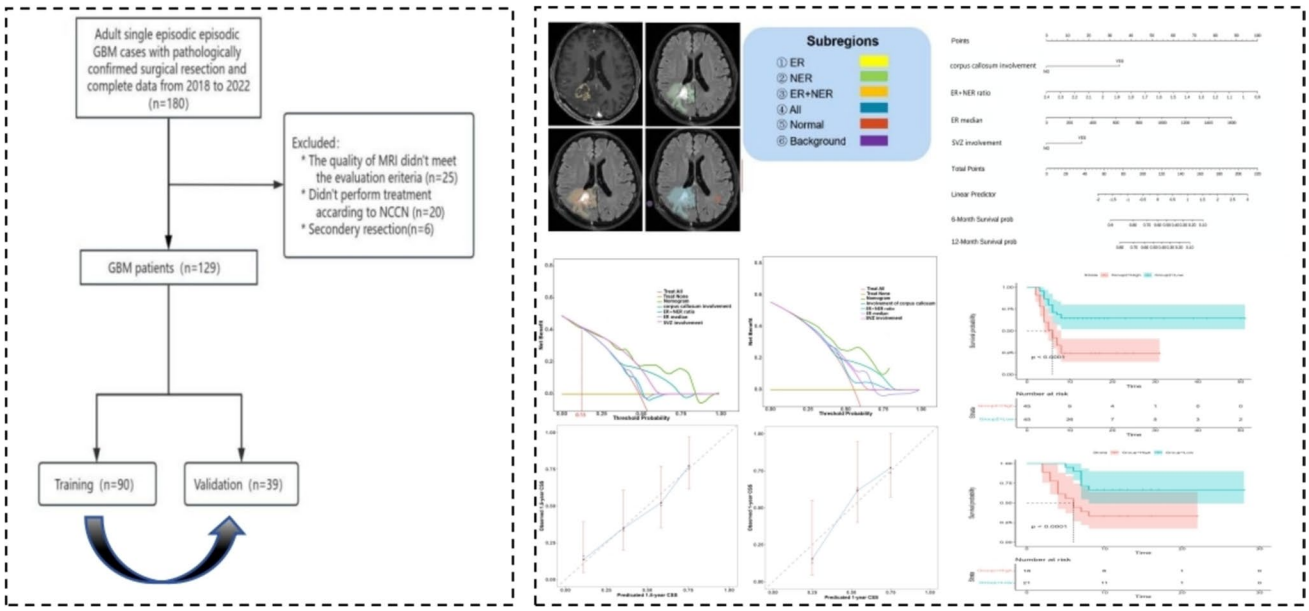

Fig. 1 The study flowchart and the radiomics workflow

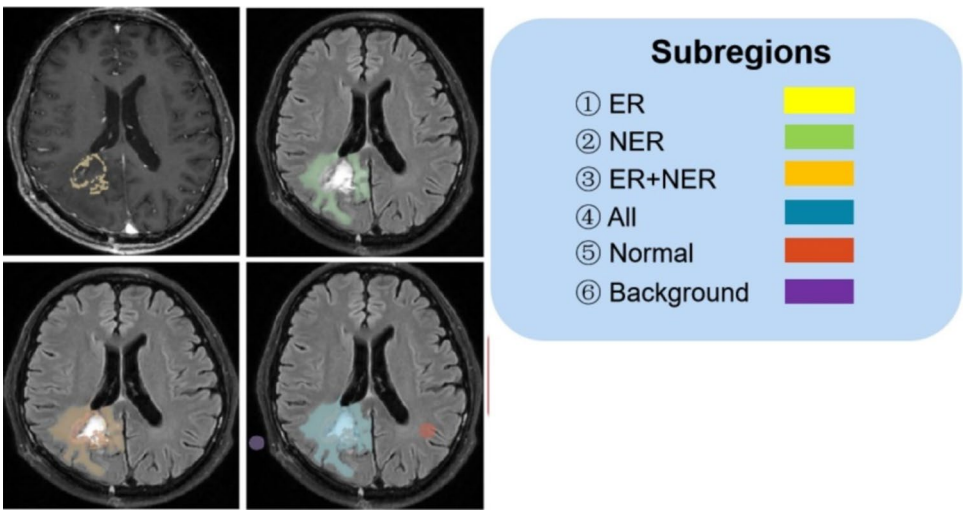

Fig. 2 Subregions of six ROIs. ER, enhancing region outside the residual cavity; NER, non-enhancement region outside the residual cavity

Statistical analysis

Interclass correlation coefficient (ICC) and kappa tests were used to evaluate inter-observer and intra-reader consistency, with values between 0.8 and 1.0 indicating excellent agreement. Statistical analyses were performed using R software and a prognostic prediction model (V3.14, Jing Ding Medical Technology Co. Ltd.). Categorical variables were compared using chi-square or Fisher exact tests, while continuous variables were analyzed using t-tests or Mann–Whitney U-tests. Results were presented as *n* (%) for categorical variables and mean ± standard deviation or median (interquartile range) for continuous variables. A sequential analysis approach was conducted to determine significant factors associated with PFS.

Significant factors from univariate Cox analysis were further evaluated using LASSO analysis for multivariate analysis. Before applying LASSO, the data were checked to ensure they met the necessary assumptions for regression analysis, such as linearity, independence, and proportional hazards. To address multicollinearity, variance inflation factors (VIFs) were examined and variables with high VIFs were either removed or combined to reduce redundancy. The results of the Cox regression analysis were used to create a nomogram using the RMS package (version 4.2.1) in R software (https://cran.r-project.org/). The predicted probability (defined as Nomo-score) of each patient was calculated

using the nomogram algorithm (with the nomogram Ex software package). The C-index was used to assess the nomogram's predictive ability, while calibration curves were used to compare predicted and observed probabilities. Decision curve analysis was performed to assess the net benefits and performance of the nomogram. The area under the curve (AUC) of the time-dependent receiver operating characteristic (ROC) curve was calculated to evaluate the model's prediction efficiency. Patients were stratified into recurrence risk categories using nomogram scores, and survival curves were compared using the log-rank test, with $P < 0.05$ considered statistically significant.

Results

General information

During the study period, a total of 180 adult GBM patients were evaluated. Of these, 51 patients were excluded for the following reasons: poor imaging quality ($n = 25$), non-adherence to NCCN treatment guidelines ($n = 20$), and secondary resection ($n = 6$). Consequently, 129 patients were included in the final analysis, comprising 52 females and 77 males, with ages ranging from 18 to 73 years (mean age: 54 years). Among these patients, 69 experienced recurrence during the study period. The patients were randomly assigned to either a training cohort ($n = 90$) or a validation cohort ($n = 39$) at a ratio of 7:3 (Table S2).

Post-operative MRI characteristics

Regarding MRI morphological characteristics, patients in the recurrence group exhibited a significantly greater midline structures displacement ($p = 0.017$) compared to those in the non-recurrence groups. However, no significant differences were observed between the two groups in terms of tumor location ($p = 0.315$), corpus callosum involvement ($p = 0.817$), residual cavity type ($p = 1.000$), enhanced region (ER) volume ($p = 0.175$), unenhanced region (NER) volume ($p = 0.367$), residual cavity morphology ($p = 0.204$), enhanced pattern ($p = 0.689$), extent of resection ($p = 0.502$), and SVZ involvement ($p = 0.061$). For subregional quantitative mertics, significant differences were noted in ER_{mean} ($p = 0.007$), ER_{median} ($p = 0.003$), and $NER_{standard\ deviation}$ ($p = 0.03$) between the recurrence and non-recurrence groups (Table 1).

For the evaluation of MRI features, the Kappa values for inter-observer agreement between the two radiologists were as follows: tumor location (0.955), corpus callosum involvement (0.931), midline shift (0.967), MAR (0.934), residual cavity type (0.943), type of residual cavity enhancement (0.921), extent of surgical resection (0.944), and SVZ involvement (0.967).

Outcome

Univariate analysis in the training cohort identified 12 clinical variables and MRI features as significant factors of recurrence, including SVZ involvement ($p = 0.047$), corpus callosum involvement ($p = 0.001$), occipital lobe location ($p = 0.001$), NER_{minmum} ($p = 0.004$), $NER_{standard\ deviation}$ ($p = 0.042$), NER_{median} ($p = 0.01$), $NER_{maximum}$ ($p = 0.008$), NER_{mean} ($p = 0.009$), ER_{median} ($p = 0.004$), ER_{mean} ($p = 0.008$), $ER_{maximum}$ ($p = 0.016$), and ER + NER rFLAIR values ($p = 0.042$). Based on LASSO regression analysis, six potential predictive factors were selected: corpus callosum involvement, SVZ involvement, ER_{median}, $ER + NER_{ratio}$, $NER_{standard\ deviation}$, and occipital lobe location (Fig. 3). Ultimately, multivariate analysis identified four significant independent variables: SVZ involvement ($p = 0.131$), ER_{median} ($p = 0.02$), $ER + NER_{ratio}$ ($p = 0.08$), and corpus callosum involvement ($p = 0.001$) (Table 2).

Nomogram model development and prediction efficiency

Significant variables from the multivariate analysis were incorporated into a nomogram model (Fig. 4A). The C-index was calculated as 0.733 for the training cohort and 0.746 for the validation cohort. The nomogram was compared with various independent variables for predicting recurrence, including corpus callosum involvement, ER + NER rFLAIR values, ER_{median}, SVZ involvement, and the nomogram score (Table 3). Two representative GBM patient cases are illustrated in Fig. 5.

The AUCs for predicting recurrence in the training group were as follows: clinical model 0.650, conventional MRI model 0.700, FLAIR value model 0.793, clinical + conventional MRI model 0.743, nomogram model 0.806, and the combined model 0.866. The AUCs in the validation cohort were: clinical model 0.536, conventional MRI model 0.799, FLAIR value model 0.531, clinical + conventional MRI model 0.813, nomogram model 0.818, and combined model 0.732 (Table S3).

Decision curve analysis showed that the nomogram score provided the greatest benefit when the threshold probability was above 0.13, with the highest net gain compared to other predictors. Calibration curves demonstrated good agreement between predicted and actual 1-year recurrence rates in both the training and validation cohorts using the nomogram with quantitative metrics derived from FLAIR hyperintensity subregions (Fig. 4B–E).

Based on a Nomogram cut-off score of 112.69, GBM patients were stratified into high- and low-risk levels.

Table 1 Characteristics of patients with GBM in the training and validation cohorts (n = 129 patients)

Characters	Training cohort ($n=90$)		*P* value	Validation cohort ($n=39$)		*P* value
	No recurrence (n = 40)	Recurrence (n = 50)		No recurrence ($n=20$)	Recurrence ($n=19$)	
Location			0.315			1.000
Frontal lobe	13 (32.5%)	17 (34.0%)		6 (30.0%)	5 (26.3%)	
Other	27 (67.5%)	33 (66.0%)		14 (70.0%)	14(73.7%)	
Corpus callosum involvement			0.817			0.065
Yes	5 (12.5%)	22 (44.0%)		3 (15.0%)	9 (47.4%)	
Midline shift			0.017			0.480
Yes	16 (40.0%)	20 (40.0%)		4 (20.0%)	6 (31.6%)	
MAR			1.000			0.910
RC type	25 (62.5%)	28 (56.0%)		14 (70.0%)	12 (63.2%)	
ER vloume	6.00 [1.75;9.00]	7.00 [3.00;11.0]	0.175	2.50 [1.00;8.25]	8.00 [5.00;12.5]	0.025
NER vloume	25.5 [12.0;48.2]	30.5 [16.2;47.5]	0.367	18.0 [12.2;25.2]	30.0 [18.0;42.5]	0.007
ER ratio	1.19 [1.00;1.34]	1.19 [1.00;1.37]	0.804	1.14 [1.00;1.50]	1.23 [1.13;1.38]	0.391
NER ratio	1.46 [1.34;1.59]	1.41 [1.32;1.51]	0.289	1.46 [1.34;1.56]	1.44 [1.35;1.54]	0.746
ER + NER ratio	1.36 [1.31;1.53]	1.34 [1.23;1.45]	0.120	1.43 (0.21)	1.39 (0.21)	0.512
All ratio	1.42 [1.27;1.61]	1.37 [1.23;1.57]	0.540	1.28 (0.36)	1.42 (0.26)	0.153
ER_{min}	93.0 [40.0;180]	93.0 [37.2;165]	0.667	70.0 [31.5;185]	91.0 [37.5;152]	0.888
ER_{max}	572 [467;846]	832 [525;1126]	0.050	665 (431)	767 (271)	0.380
ER_{mean}	325 [257;507]	489 [318;671]	0.007	299 [264;556]	357 [334;547]	0.227
ER_{median}	312 [248;497]	500 [314;682]	0.003	298 [251;562]	341 [306;562]	0.318
$ER_{standard\ deviation}$	93.2 [70.5;136]	118 [78.6;173]	0.108	110 (75.2)	125 (55.5)	0.483
NER_{min}	324 [296;464]	458 [303;667]	0.073	336 [264;556]	336 [304;572]	0.633
NER_{max}	542 [462;687]	777 [494;1074]	0.057	628 [475;1044]	640 [528;836]	0.768
NER_{mean}	394 [364;574]	627 [360;806]	0.085	401 [330;691]	416 [373;671]	0.448
NER_{median}	386 [359;569]	611 [351;795]	0.092	392 [325;676]	392 [364;666]	0.482
$NER_{standard\ deviation}$	38.4 [26.9;48.8]	49.9 [35.0;73.4]	0.030	52.6 [32.4;74.1]	49.3 [35.9;72.7]	0.888
RC morphology			0.204			0.149
Irregular	13 (32.5%)	24 (48.0%)		5 (25.0%)	10 (52.6%)	
Enhanced pattern			0.689			0.077
II	19 (47.5%)	27 (54.0%)		7 (35.0%)	13 (68.4%)	
Extent of resection			0.502			0.182
Total	37 (92.5%)	43 (86.0%)		19 (95.0%)	15 (78.9%)	
SVZ involvement			0.061			0.020
SVZ +	22 (55.0%)	38 (76.0%)		12 (60.0%)	18 (94.7%)	

GBM glioblastoma, *RC* residual cavity, *ER* enhancing region outside the residual cavity, *NER* non-enhancing region outside the residual cavity, *SVZ* subventricular zone, *KPS* Karnofsky Performance Scale

Approximately 50% of patients were classified as high-risk level. Kaplan–Meier curves analysis revealed that patients in the low-risk level had a significantly lower recurrence rate compared to those in the high-risk level ($p<0.001$ for the training cohort, $p=0.025$ for the validation cohort) (Fig. 4F, G).

Discussion

In the present study, we developed a nomogram model for personalized prediction of recurrence in adult GBM patients using quantitative metrics from segmented

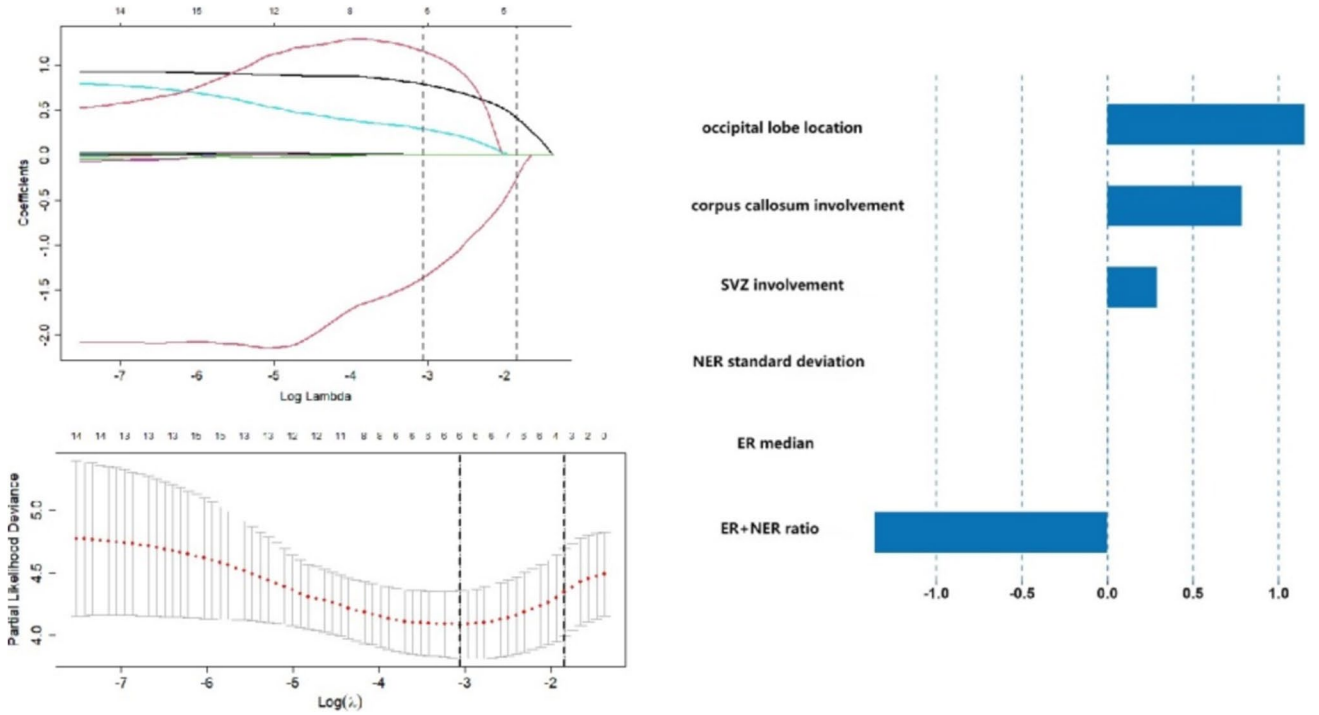

Fig. 3 **A** LASSO feature selection and tuning, where the vertical dashed line indicated the optimal penalty coefficient λ corresponding to the non-zero features. **B** The AUC curve plotted through tenfold cross-validation, with the dashed lines on the left and right representing λ min and λ 1se, respectively. λ min was selected for this study. **C** The 6 features retained after LASSO filtering and their respective weight coefficients

Table 2 Univariate and multivariate analyses for unfavorable PFS of training cohort

Characteristics	Univariate analysis		Multivariate analysis	
	HR (95%CI)	*P* value	HR (95%CI)	*P* value
SVZ involvement	1.934 [1.009–3.706]	0.047	1.671 [0.859–3.25]	0.131
NER_{sd}	1.008 [1–1.016]	0.042		
NER_{median}	1.001 [1–1.003]	0.01		
NER_{max}	1.001 [1–1.002]	0.008		
NER_{mean}	1.001 [1–1.003]	0.009		
NER_{min}	1.002 [1.001–1.003]	0.004		
ER_{median}	1.001 [1–1.002]	0.004	1.002 [1.001–1.003]	0.002
ER_{mean}	1.001 [1–1.002]	0.008		
ER_{max}	1.001 [1–1.001]	0.016		
ER + NER ratio	0.227 [0.054–0.948]	0.042	0.142 [0.034–0.598]	0.008
Occipital lobe location	13.018 [2.686–63.079]	0.001		
Corpus callosum involvement	2.63 [1.498–4.616]	0.001	2.74 [1.5–5.003]	0.001

HR Hazard ratio, *95% CI* 95% confidence interval, *ER* enhancing region outside the residual cavity, *NER* non-enhancing region outside the residual cavity, *SVZ* subventricular zone

subregions on pre-CRT FLAIR-CET1WI fusion images. Our preliminary findings indicate that specific quantitative metrics from subregions, along with certain conventional MRI morphologic features, were significant risk factors for early GBM recurrence. These metrics included the ER_{median} and ER + NER rFLAIR values, and the involvement of SVZ and corpus callosum. Pre-CRT MRI-based nomograms outperformed clinical and conventional MRI models in prognostic assessment, demonstrating greater accuracy and predictive performance. To the authors' knowledge, no previous studies have focused on early recurrence prediction using quantitative metrics

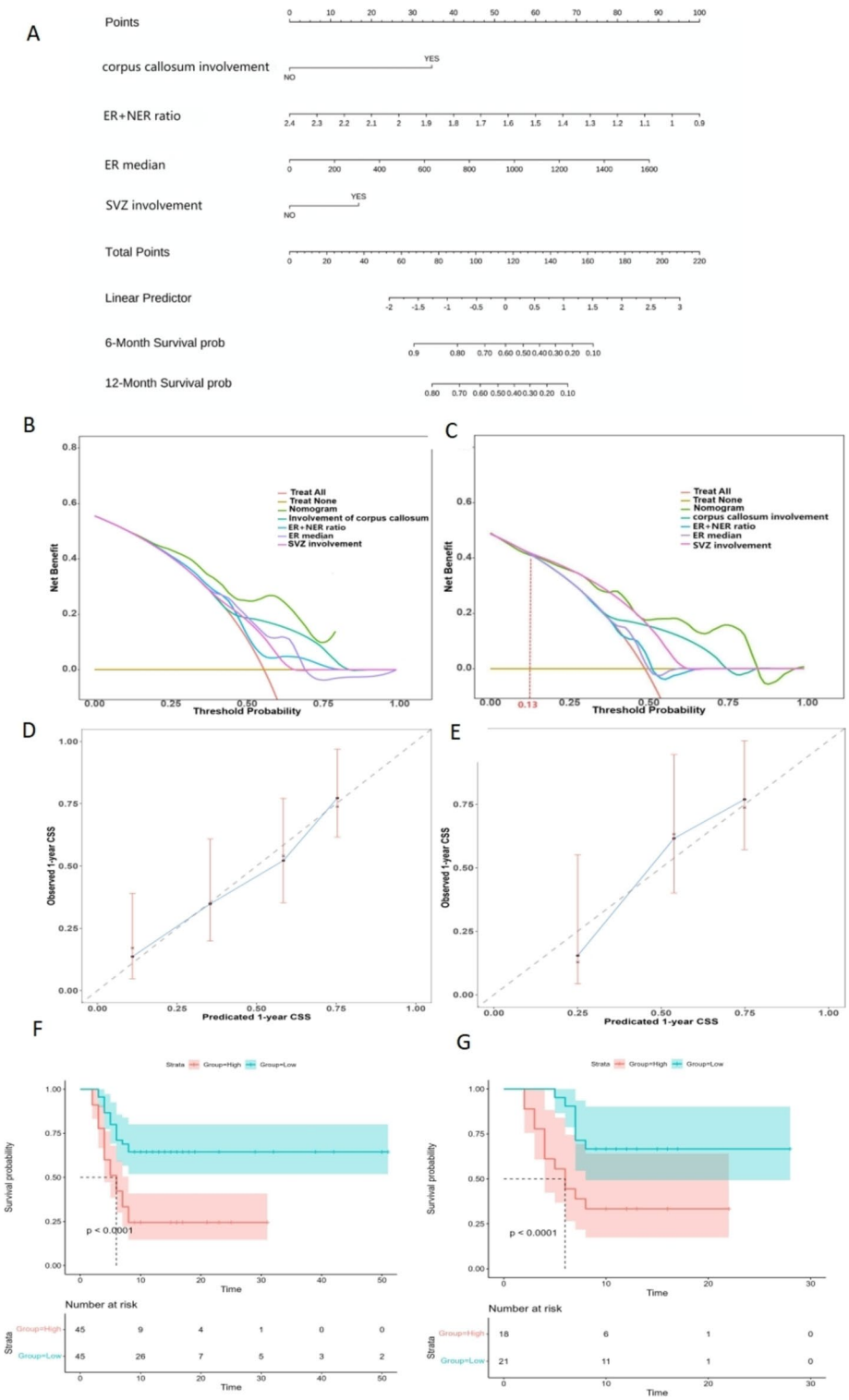

Fig. 4 The combined model was constructed and presented as a nomogram. **A** Decision curve analysis of the nomogram score and each independent predictor predicting PFS in the training (**B**) and validation (**C**) cohorts. The y-axis represents net benefit, and the x-axis represents threshold probability. Decision curves show that when the threshold probability is greater than 0.13 (red dotted line), the column-line graph (green line) has more benefit than all patients with a positive clinical outcome (red line) or no positive clinical outcome (brown line). Calibration plots of the nomogram. The diagonal line indicates the ideal value, and the solid line represents the performance of the nomogram; the closer the solid line is to the diagonal dashed line, the better the calibration will be. The calibration curves demonstrated good calibration of the nomogram in the training group (**D**) and validation group (**E**). Kaplan–Meier curves based on the Nomo-score (cut-off value of 112.69) for PFS in GBM patients (**F**, **G**). PFS, progression-free survival. GBM, glioblastoma. ER, enhancing region outside the residual cavity; NER, non-enhancement region outside the residual cavity

based on segmented MRI fusion images and nomogram models.

This study has several advantages, including predicting early GBM recurrence using pre-CRT MRI data (which minimizes the influence of surgical procedures), extracting factors from conventional MRI sequence, identifying novel imaging markers for early warnings, and utilizing open software for image fusion. Furthermore, postoperative and pre-CRT MRI are less affected by residual hemorrhage around the surgical cavity. Previous studies had shown that FLAIR SI can be used to differentiate GBM from solitary brain metastasis (Nguyen et al. 2022). However, exploration

Table 3 The C-index of prognostic factors and nomogram for prediction PFS in the training and validation cohorts

Models	C-index (95% confidence interval)	
	Training cohort	Validation cohort
Corpus callosum involvement	0.621 (0.554–0.688)	0.664 (0.558–0.77)
ER + NER ratio	0.577 (0.491–0.663)	0.563 (0.42–0.706)
ER_{median}	0.648 (0.568–0.728)	0.545 (0.406–0.684)
SVZ involvement	0.581 (0.514–0.648)	0.64 (0.562–0.718)
ER + NER ratio + ER_{median}	0.608 (0.53–0.686)	0.735 (0.613–0.857)
Nomogram	0.733 (0.659–0.807)	0.746 (0.642–0.85)

PFS progression free survival, *ER* enhancing region outside the residual cavity, *NER* non-enhancing region outside the residual cavity, *SVZ* subventricular zone, *C index* concordance index

in predicting GBM recurrence with this method remains limited. Since pre-CRT imaging could help to predict post-treatment reactions such as pseudo-progression and pseudo-remission (Amidon et al. 2022), identifying new imaging markers and developing new methods based on conventional MRI sequences like FLAIR could be valuable for early warning of recurrence and timely implementation of salvage treatment, thereby improving survival outcomes for GBM patients.

One challenge with purely morphological analysis is distinguishing between cerebral edema, ischemia, and residual tumor tissue in FLAIR hyperintensity areas (Broggi et al. 2023). Since visual differentiating SI can be challenging, quantitative SI measurements could help to identify areas with residual tumor cells (Long et al. 2023). Previous studies had reported differences in FLAIR SI between areas of recurrence and non-recurrence shortly after surgery (1–8 days) (Chang et al. 2017), suggesting that increased SI may serve as an earlier indicator of tumor progression, with more prediction efficiency than the volume increase of FLAIR hyperintensity lesions. Investigating FLAIR hyperintensity areas based on segmented subregions could lead to a better understanding of their underlying pathology. Although previous studies have explored the relationship between FLAIR quantitative metrics and survival in low-grade gliomas (Yuan et al. 2022), research on GBM has been limited. The present study shows that quantitative metrics based on segmented FLAIR-CET1WI fusion images can improve the efficiency of predicting GBM recurrence risk. The pre-CRT FLAIR hyperintensity metrics, including both ER_{median} and ER + NER rFLAIR values, were significant predictors of tumor recurrence. A lower rFLAIR value of the hyperintensity subregions surrounding residual cavity was associated with earlier tumor recurrence, consistent with previous studies. For instance, in a study of 26 GBM patients post-surgery (Chang et al. 2017), a negative correlation was found between FLAIR SI and tumor cell counts, along with an association between rFLAIR values and shorter PFS. Thus, these quantitative metrics could be helpful in predicting GBM recurrence.

Our preliminary results confirmed the utility of conventional MRI features in predicting GBM recurrence, including SVZ and corpus callosum involvement. Both SVZ (Huang et al. 2021a, b; Adeberg et al. 2022) and corpus callosum involvement (Fyllingen et al. 2021; Hazaymeh et al. 2022) are independent risk factors for GBM recurrence. SVZ involvement promotes tumor stem cell formation and differentiation (Loras et al. 2023), while corpus callosum involvement facilitates tumor cell migration to the opposite hemisphere. Patients with corpus callosum involvement exhibit higher changes in platelet-derived growth factor receptor alpha, correlating with lower survival rates (Cui et al. 2022). However, previous studies focused on preoperative MRI morphologic metrics (Huang et al. 2021a, b; Adeberg et al. 2022; Fyllingen et al. 2021; Hazaymeh et al. 2022), and the relationship between abnormal SI surrounding residual cavity, SVZ and/or corpus callosum involvement, and GBM recurrence before CRT remains underexplored. We further investigated the predictive value of post-operative conventional MRI features around the residual cavity. The preliminary results demonstrated that combining quantitative metrics extracted from FLAIR hyperintensity subregions with conventional MRI features improves predictive efficiency.

Nomogram is valuable tool for individualized prediction of GBM recurrence risk, confirming their usefulness in oncology. In constructing the nomogram model, scores were assigned based on each predictor's contribution. The scores of the enrolled variables were summed to produce a total score, which represents the precise probability of tumor recurrence. The advantage of nomograms is their ability to simplify complex regression equations into visual representations, enabling easy interpretation and digitization of results, thus supporting personalized decision-making (Tunthanathip et al. 2021). Nomograms are widely used in clinical settings for predicting disease risk or prognosis, including glioma. A previous study (Xie and Li 2022) confirmed the effectiveness of a nomogram in assessing GBM prognosis by creating a model based on preoperative imaging and histological features to predict glioma recurrence within 1 year after tumor resection. In Zheng's study, the nomogram, which incorporated preoperative imaging features as well as clinical and molecular variables, improved predictive accuracy of PFS in GBM patients (Zheng et al. 2021). Comparatively, our study extracted quantitative metrics from conventional MRI sequence at pre-CRT and post-operative time points, allowing us to evaluate the impact of postoperative changes on prediction efficiency.

Limitations of this study should be noted. First, the small sample size, due to the exclusion of multiple lesions and the

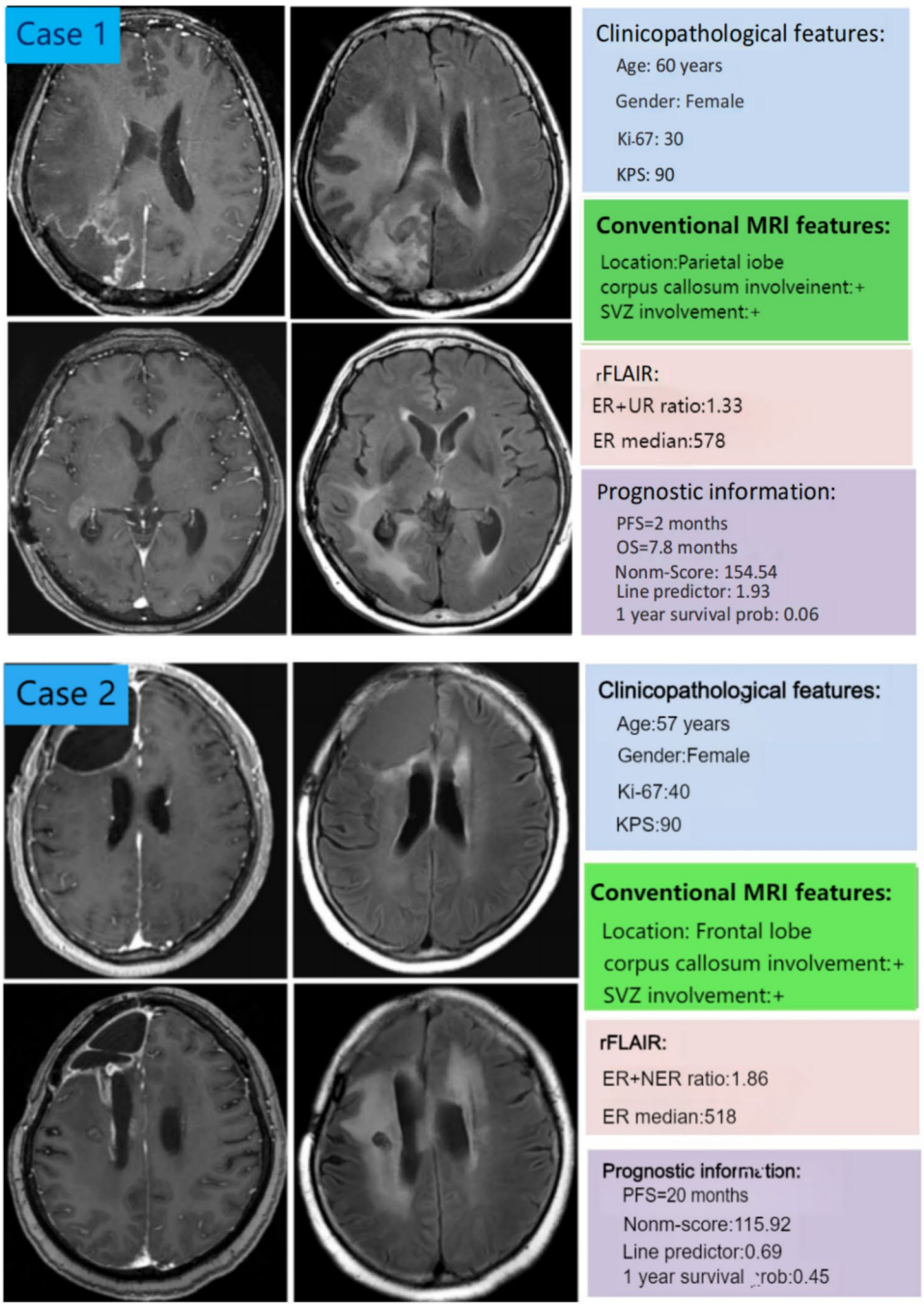

Fig. 5 Two presented cases of GBM patients who had distinctly different PFS time (2 months vs. 15 months) with similar clinic pathological features showed significantly different nomo-scores (154.54 vs. 115.92; $P < 0.001$). PFS, progression free survival; OS, overall survival; ER, enhanced regional outside the residual cavity; NER, non-enhancement region outside the residual cavity; SVZ, subventricular zone

impact of surgical resection on recurrence and prognosis (Jackson et al. 2020; Di et al. 2022), may result in selective bias. Future studies with larger external validation cohorts are needed to confirm the findings. Second, long-term follow-up is necessary to differentiate tumor infiltration from true cerebral edema and ischemia. Future studies should integrate functional MRI, including diffusion weighted imaging (DWI), perfusion weighted imaging (PWI), and MR spectroscopy (MRS) to address this limitation. Previous studies have demonstrated the utility of functional imaging in evaluating peri-tumoral FLAIR hyperintensity subregions (Yan et al. 2017). The apparent diffusion coefficient value in peri-tumor regions could be used to create nomogram models for predicting glioma progression (Pala et al. 2021). Additionally, DTI, MR spectroscopy, and positron emission tomography have been reported to be useful in delineating the "true" boundaries of this aggressive tumor, thereby further improving patient prognosis (Price and Gillard 2011). We speculate that incorporating functional sequences into the pre-radiotherapy imaging protocol for GBM patients could enhance prognostic prediction, which will be a key focus of future prospective studies.

Conclusion

In conclusion, the quantitative metrics of the hyperintensity subregion surrounding the residual cavity on FLAIR were independent predictors of GBM recurrence. FLAIR-CET1WI image fusion is essential for this subregional segmentation. The metrics extracted from fusion images, when combined with conventional MRI morphological features, could be used to successfully construct a nomogram model. This novel nomogram model would effectively improve the prediction of early GBM recurrence. However, further multicenter studies enrolling multimodal functional MRI techniques for constructing nomograms should be conducted to enhance individualized prediction efficiency and validate the value of this method, providing a novel approach for early detection of GBM recurrence.

Supplementary Information The online version contains supplementary material available at https://doi.org/10.1007/s00432-024-06008-6.

Author contributions All authors contributed to the study conception and design. Material preparation, data collection, and analysis were performed by YT, YXY. The first draft of the manuscript was written by GLJ and all authors commented on previous versions of the manuscript. We invited Professor LYW to review the manuscript and verify the results. The project was guided by QGM and LYM. All authors read and approved the final manuscript.

Funding The authors declare that no funds, grants, or other support were received during the preparation of this manuscript.

Data availability No datasets were generated or analysed during the current study.

Declarations

Conflict of interests The authors declare no competing interests.

Ethics approval This study was performed in line with the principles of the Declaration of Helsinki. Approval was granted by the Ethics Committee of The second hospital of Hebei Medical University (Date 2024.3.8/No.2024-R186).

Consent to participate Informed consent was obtained from all individual participants included in the study.

Consent to publish The authors affirm that human research participants provided informed consent for publication of the images in Fig. 5.

References

Adeberg S, Knoll M, Koelsche C et al (2022) DNA-methylome-assisted classification of patients with poor prognostic subventricular zone associated IDH-wildtype glioblastoma. Acta Neuropathol 144:129–142. https://doi.org/10.1007/s00401-022-02443-2

Amidon RF, Santos-Pinheiro F, Straza M et al (2022) Case report: fractional brain tumor burden magnetic resonance imageping to assess response to pulsed low-dose-rate radiotherapy in newly-diagnosed glioblastoma. Front Oncol 12:1066191. https://doi.org/10.3389/fonc.2022.1066191

Behling F, Rang J, Dangel E et al (2022) Complete and incomplete resection for progressive glioblastoma prolongs post-progression survival. Front Oncol 12:75543. https://doi.org/10.3389/fonc.2022.755430

Bender K, Träger M, Wahner H et al (2021) What is the role of the subventricular zone in radiotherapy of glioblastoma patients? Radiother Oncol 158:138–145. https://doi.org/10.1016/j.radonc.2021.02.017

Broggi G, Altieri R, Barresi V et al (2023) Histologic definition of enhancing core and FLAIR hyperintensity region of glioblastoma, IDH-wild type: a clinico-pathologic study on a single-institution series. Brain Sci 13:248. https://doi.org/10.3390/brainsci13020248

Chang PD, Chow DS, Yang PH et al (2017) Predicting glioblastoma recurrence by early changes in the apparent diffusion coefficient value and signal intensity on FLAIR images. Am J Roentgenol 208:57–65. https://doi.org/10.2214/AJR.16.16234

Chen L, Chen R, Li T et al (2023) Multi-parameter MRI based radiomics nomogram for predicting telomerase reverse transcriptase promoter mutation and prognosis in glioblastoma. Front Neurol 14:1266658. https://doi.org/10.3389/fneur.2023.1266658

Chiang GC, Pisapia DJ, Liechty B et al (2020) The prognostic value of MRI subventricular zone involvement and tumor genetics in lower grade gliomas. J Neuroimaging 30:901–909. https://doi.org/10.1111/jon.12763

Cui M, Chen H, Sun G et al (2022) Combined use of multimodal techniques for the resection of glioblastoma involving corpus callosum. Acta Neurochir 164:689–702. https://doi.org/10.1007/s00701-021-05008-6

Di L, Shah AH, Mahavadi A et al (2022) Radical supramaximal resection for newly diagnosed left-sided eloquent glioblastoma: safety and improved survival over gross-total resection. J Neurosurg 138:62–69. https://doi.org/10.3171/2022.3.JNS212399

Du P, Yang X, Shen L et al (2022) Nomogram model for predicting the prognosis of high-grade glioma in adults receiving standard treatment: a retrospective cohort study. J Clin Med 12:196. https://doi.org/10.3390/jcm12010196

Fyllingen EH, Bø LE, Reinertsen I et al (2021) Survival of glioblastoma in relation to tumor location: a statistical tumor atlas of a population-based cohort. Acta Neurochir 163:1895–1905. https://doi.org/10.1007/s00701-021-04802-6

García Vicente AM, Amo-Salas M, Sandoval Valencia H et al (2022) Early recurrence detection of glioma using 18 F-Fluorocholine PET/CT: GliReDe pilot study. Clin Nucl Med 47:856–862. https://doi.org/10.1097/RLU.0000000000004329

Hazaymeh M, Löber-Handwerker R, Döring K et al (2022) Prognostic differences and implications on treatment strategies between butterfly glioblastoma and glioblastoma with unilateral corpus

callosum infiltration. Sci Rep 12:19208. https://doi.org/10.1038/s41598-022-23794-6
Huang WY, Wen LH, Wu G et al (2021a) Radiological model based on the standard magnetic resonance sequences for detecting methylguanine methyltransferase methylation in glioma using texture analysis. Cancer Sci 112:2835–2844. https://doi.org/10.1111/cas.14918
Huang R, Wang T, Liao Z et al (2021) A retrospective analysis of the risk factors affecting recurrence time in patients with recurrent glioblastoma. Ann Palliat Med 10:5391–5399. https://doi.org/10.21037/apm-21-823
Jackson C, Choi J, Khalafallah AM et al (2020) A systematic review and meta-analysis of supratotal versus gross total resection for glioblastoma. J Neurooncol 148:419–431. https://doi.org/10.1007/s11060-020-03556-y
Jia X, Zhai Y, Song D et al (2022) A multiparametric MRI-based radiomics nomogram for preoperative prediction of survival stratification in glioblastoma patients with standard treatment. Front Oncol 12:758622. https://doi.org/10.3389/fonc.2022.758622
Long H, Zhang P, Bi Y et al (2023) MRI radiomic features of peritumoral edema may predict the recurrence sites of glioblastoma multiforme. Front Oncol 12:1042498. https://doi.org/10.3389/fonc.2022.1042498
Loras A, Gonzalez-Bonet LG, Gutierrez-Arroyo JL et al (2023) Neural stem cells as potential glioblastoma cells of origin. Life 13:905. https://doi.org/10.3390/life13040905
Nguyen DH, Nguyen DM, Nguyen HV et al (2022) Discrimination between glioblastoma and solitary brain metastasis: a quantitative analysis based on FLAIR signal intensity. Eur Rev Med Pharmacol Sci 26:3577–3584. https://doi.org/10.26355/eurrev_202205_28853
Pala A, Durner G, Braun M et al (2021) The impact of an ultra-early postoperative MRI on treatment of lower grade glioma. Cancers 13:2914. https://doi.org/10.3390/cancers13122914
Price SJ, Gillard JH (2011) Imaging biomarkers of brain tumour margin and tumour invasion. Br J Radiol 84:S159–S167. https://doi.org/10.1259/bjr/26838774
Rao C, Jin J, Lu J et al (2022) A multielement prognostic nomogram based on a peripheral blood test, conventional MRI and clinical factors for glioblastoma. Front Neurol 13:822735. https://doi.org/10.3389/fneur.2022.822735
Tunthanathip T, Ratanalert S, Sae-Heng S et al (2021) Prognostic factors and clinical nomogram predicting survival in high-grade glioma. J Cancer Res Ther 17:1052–1058. https://doi.org/10.4103/jcrt.JCRT_233_19
Wang S, Xiao F, Sun W et al (2022) Radiomics analysis based on magnetic resonance imaging for preoperative overall survival prediction in isocitrate dehydrogenase wild-type glioblastoma. Front Neurosci 15:791776. https://doi.org/10.3389/fnins.2021.791776
Wen PY, van den Bent M, Youssef G et al (2023) RANO 2.0: update to the response assessment in neuro-oncology criteria for high- and low-grade gliomas in adults. J Clin Oncol 41:5187–5199. https://doi.org/10.1200/JCO.23.01059
Wu G, Shi Z, Chen Y et al (2019) A sparse representation-based radiomics for outcome prediction of higher grade gliomas. Med Phys 46:250–261. https://doi.org/10.1002/mp.13288
Xie G, Li K (2022) A nomogram based on MRI and radiomics for prediction of postoperative recurrence of glioma. J Clin Radiol 41:1814–1818. https://doi.org/10.13437/j.cnki.jcr.2022.10.022
Yamaki T, Shibahra I, Matsuda KI et al (2020) Relationships between recurrence patterns and subventricular zone involvement or CD133 expression in glioblastoma. J Neurooncol 146:489–499. https://doi.org/10.1007/s11060-019-03381-y
Yan JL, Li C, van der Hoorn A et al (2020) Publisher correction: a neural network approach to identify the peritumoral invasive areas in glioblastoma patients by using MR radiomics. Sci Rep 10:13808. https://doi.org/10.1038/s41598-020-70346-x
Yan JL, van der Hoorn A, Larkin TJ et al (2017) Extent of resection of peritumoral diffusion tensor imaging-detected abnormality as a predictor of survival in adult glioblastoma patients. J Neurosurg 126:234–241. https://doi.org/10.3171/2016.1.JNS152153
Yuan T, Gao Z, Wang F et al (2022) Relative T2-FLAIR signal intensity surrounding residual cavity is associated with survival prognosis in patients with lower-grade gliomas. Front Oncol 12:960917. https://doi.org/10.3389/fonc.2022.9609
Zhang JF, Okai B, Iovoli A et al (2024) Bevacizumab and gamma knife radiosurgery for first-recurrence glioblastoma. J Neurooncol 166:89–98. https://doi.org/10.1007/s11060-023-04524-y
Zheng L, Zhou ZR, Shi M et al (2021) Nomograms for predicting progression-free survival and overall survival after surgery and concurrent chemoradiotherapy for glioblastoma: a retrospective cohort study. Ann Transl Med 9:571. https://doi.org/10.21037/atm-21-673